

A DESIGN OF MINIATURIZED ULTRA-WIDEBAND PRINTED SLOT ANTENNA WITH 3.5/5.5 GHz DUAL BAND-NOTCHED CHARACTERISTICS: ANALYSIS AND IMPLEMENTATION

Mohamed Mamdouh M. Ali^{1, *}, Ayman Ayd R. Saad², and
Elsayed Esam M. Khaled¹

¹Electrical Engineering Department, Assiut University, Assiut, Egypt

²Electrical Engineering Department, South Valley University, Qena,
Egypt

Abstract—A design and analysis of a novel proximity-fed printed slot antenna with 3.5/5.5 GHz dual band-notched characteristics are presented. To obtain an ultra-wideband (UWB) response, a circular patch with a rectangular conjunction arm is etched concentrically inside a ground plane aperture. The antenna is proximity-fed by a microstrip line with an open shunt stub on the other side of the substrate. The designed antenna satisfies a -10 dB return loss requirement in the frequency band from 2.7 to 17 GHz. In order to obtain dual band-notched properties at 3.5 and 5.5 GHz, an open ring slot is etched off the circular patch and a π -shaped slot is etched off the microstrip feeding line, respectively. A curve fitting formulation is obtained to describe the influences of the notched resonators on the corresponding notched frequencies. The proposed antenna is designed, simulated and fabricated. The measured data show a good agreement with the simulated results and the equivalent circuit results through the use of a modified Vector Fitting technique for a rational function approximation. The proposed antenna provides almost omnidirectional radiation patterns, relatively flat gain and high radiation efficiency over the entire UWB frequency excluding the two rejected bands.

Received 13 April 2013, Accepted 10 May 2013, Scheduled 21 May 2013

* Corresponding author: Mohamed Mamdouh M. Ali (mohamedmmdouh981@yahoo.com).

1. INTRODUCTION

Recently, UWB communication system is attracting more and more attention because of its advantages such as low power consumption, high data rate transmissions as in the multimedia communications, robustness against jamming, and high degree of reliability. In 2002, the Federal Communication Commission (FCC) officially released the regulations for UWB technology with allocated spectrum from 3.1 to 10.6 GHz for unlicensed UWB indoor medical, measurement and communication applications [1]. Consequently, an increased interest and intensive research work have been reported to the UWB antenna design.

A problem of using the UWB in public applications is that the frequency range for UWB systems will cause interference to the existing wireless communication systems, such as the IEEE 802.16 standard for WiMAX system at 3.5 GHz (3.3–3.7 GHz) and the IEEE 802.11a standard for WLAN system at 5.5 GHz (5.15–5.825 GHz). In order to avoid such interferences along these bands, a UWB antenna with multiple band-notched characteristics is required. Various methods have been proposed and developed in the literature to notch-out a single- or multi-frequency band(s) [2–27].

The most popular method for a band-notching is inserting slots. Various slots have been suggested by many researchers to be inserted in the radiating element, ground plane, feeding line and vicinity of the radiating element [2–15]. The fractal structure is used to achieve both size reduction and frequency band notched characteristic in UWB antennas [16–19]. More recently, several research groups have attempted to reject certain frequency bands using the metamaterial structures such as a split ring resonator (SRR) and a complementary split ring resonator (CSRR) [20–25]. Because of these structures are electronically small resonators with very high Q_s , they can be considered as filters providing sharp notches or pass of certain frequency bands. Also electromagnetic band gap (EBG) structures are used to improve UWB antenna performance such as increasing the antenna's gain as well as produce a frequency band-notched characteristic [26, 27]. These aforementioned methods can achieve a good single or dual band-notched property, but some of them are with large size or complicated design procedure which makes them unsuitable for the UWB antennas themselves.

In this paper, we propose a novel proximity-fed UWB printed slot antenna with dual band-notched property. The proposed antenna can cover the UWB frequency range (2.7–17 GHz) and avoid interference with the 3.5 GHz band for WiMAX systems and the 5.5 GHz band for

WLAN systems with a simpler structure and smaller size than those given in the literatures. Details of the antenna design with simulation and experiment results are presented and discussed. Curve fitting formulations for fast determination of notched frequency response is obtained. Moreover, a SPICE-compatible circuit modeling of the proposed antenna is obtained and verified through the use of the modified rational function modeling technique.

2. ANTENNA DESIGN AND CONSIDERATIONS

Based on several parametric studies, the geometry of the proposed dual band-notched UWB antenna is illustrated in Figure 1. The antenna is printed on a $20(W) \times 25(L)$ mm² FR4 substrate with a relative permittivity of 4.7, a loss tangent $\tan\delta = 0.025$ and a thickness $h = 1.5$ mm. The substrate is backed by a copper ground plane of the same surface area. A circular disk radiating patch of radius $R = 5.5$ mm is placed concentrically inside a rectangular slot of a $17(W_s) \times 15(L_s)$ mm² etched off the ground plane. The center of the patch and the ground plane slot are in the same vertical symmetric line of the substrate. A rectangular conjunction arm of size $1.0(W_r) \times 3.5(L_r)$ mm² is used to connect the radiating patch with the ground plane. The circular patch is excited using a $50\ \Omega$ proximity-fed microstrip line placed on the other side of the substrate, with width $W_f = 2.0$ mm and length, $L_f = 11$ mm. The microstrip line is put on the other side of the substrate symmetrically with the vertical symmetric line of the substrate and started with the lower edge of the ground plane. To improve the impedance matching, a small rectangular slot $4.0(W_{ss}) \times 3.5(L_{ss})$ mm² is etched off the ground plane underneath the feeding line in the other side of the substrate. To further improve the impedance matching, an open stub is connected in shunt to the feeding line with dimension $2.0(W_{stub}) \times 1.0(L_{stub})$ mm² at a distance $P_{stub} = 1.0$ mm from the end of the feeding line, as shown in Figure 1(a).

To obtain dual band-notched characteristics at 3.5 GHz corresponding to WiMAX system and at 5.5 GHz corresponding to WLAN, an open ring slot is etched off the circular patch and a π -shaped slot is etched off the feeding line, respectively. The external radius of the open ring is $R_o = 5.0$ mm and its gap is $g = 1.0$ mm. The ring is of a uniform width 1.5 mm. On the other hand, the three sides of the π -shaped slot are $L_{\pi 1}$, $L_{\pi 2}$, and $L_{\pi 3}$ as shown in Figure 1(b). These lengths are optimized to control the corresponding band-notch performance. The π -shaped slot is of a uniform width 0.4 mm and of dimensions of $L_{\pi 1} = L_{\pi 2} = 8.5$ mm, and $L_{\pi 3} = 1.4$ mm. The pro-

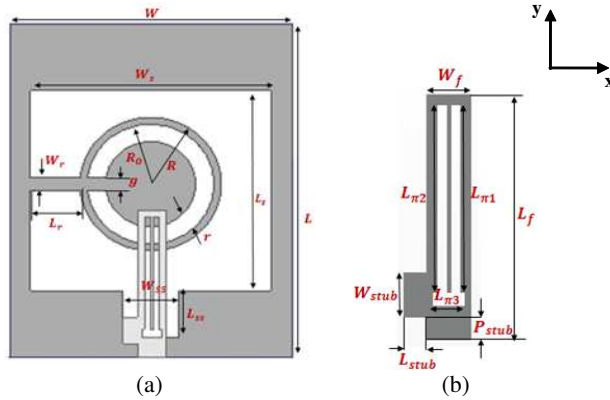


Figure 1. The proposed dual band-notched UWB antenna. (a) Geometry of the antenna. (b) Specifications of the antenna microstrip feeding line with open shunt stub.

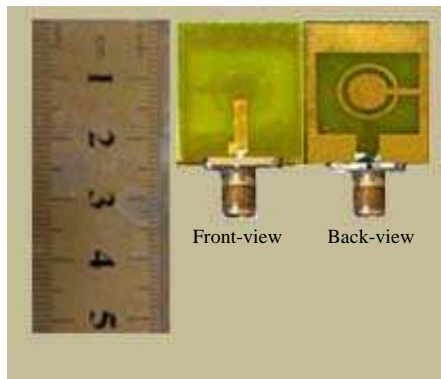


Figure 2. Photograph of the front- and back-view of the fabricated antenna.

posed antenna is fabricated after optimizing its shape, dimensions, and its notches resonators. A photograph of the implemented antenna is shown in Figure 2.

3. EFFECTS OF NOTCH PARAMETERS ON ANTENNA PERFORMANCE

The bandwidth and center frequency of the notched bands are the most important parameters of a band-notched antenna. In this Section, we

study the effects of the slots resonators on the corresponding notched-bands of the proposed antenna.

Figure 3 shows the VSWR characteristic versus frequency with different values of the external radius, R_o and the gap length, g of the open ring slot. Figure 3(a) shows that as R_o increases the band-notch shifts toward the low frequencies and the antenna bandwidth decreases. Figure 3(b) illustrates that as the g increases which means that the circumference length of the open ring decreases, the notched band shifts toward the high frequencies. It is noticed that the bandwidth of the notch frequency can be easily tuned by adjusting the radius of the ring and the length of its gap. When the external radius of the open ring slot is $R_o = 5.0$ mm and its gap is $g = 1.0$ mm, with a uniform width of 1.5 mm, the antenna bandwidth is 2.7 to 17 GHz with a sharp band rejection from 3.3 to 3.8 GHz.

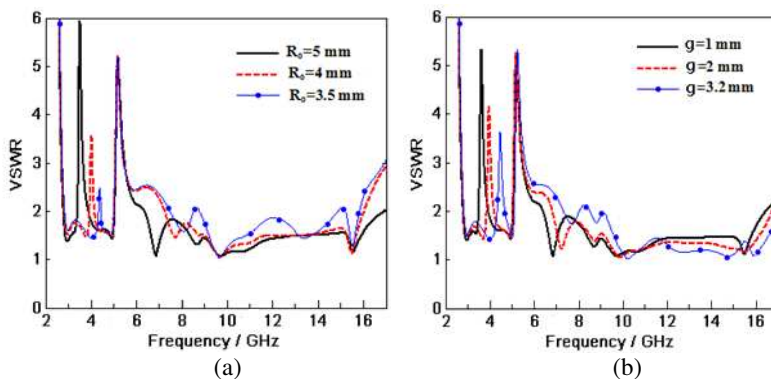


Figure 3. Simulated VSWR characteristics versus frequency of the proposed antenna with notched resonators. (a) For different values of the open ring radius, R_o . (b) For different values of the gap length, g .

Second, the effect of dimensions of the π -shaped slot integrated on the microstrip feed-line on the corresponding notched frequency at 5.5 GHz is demonstrated. The three lengths of the slot $L_{\pi 1}$, $L_{\pi 2}$, and $L_{\pi 3}$, are used to optimize the band-notch performance. Results of the simulated VSWR of the proposed antenna with different lengths of $L_{\pi t}$ are shown in Figure 4. The results illustrate that when the total length of the π -shaped slot decreases the central frequency of the band notch increases. The optimal dimensions of the π -shaped slot are $L_{\pi 1} = L_{\pi 2} = 8.5$ mm and $L_{\pi 3} = 1.4$ mm with a uniform width 0.4 mm. This optimal design gives a bandwidth from 2.7 to 17 GHz with a sharp band rejection from 5.0 to 6.1 GHz.

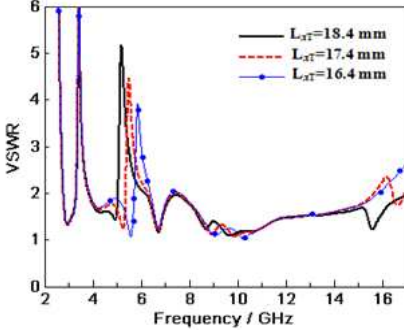


Figure 4. Simulated VSWR characteristics versus frequency of the proposed antenna with notched structures for different lengths of the π -shaped slot etched off the microstrip feeding line.

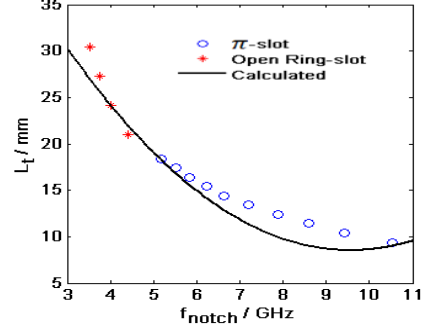


Figure 5. Comparison between the calculated and simulated values of the notched frequencies for various total slots lengths of the proposed resonators.

The proposed band-notched UWB antenna has the capability to provide easy tuning of the bandwidth with good and suitable band rejection function by dimensions adjustment of the slots resonators.

As a first order of approximation, the dimensions of the slots resonators can be chosen to be a half wavelength according to the following formula

$$L_{slot} \approx \frac{\lambda_g}{2} \quad (1)$$

The wavelength can be approximately calculated by the formulas as follows

$$\lambda_g = \frac{\lambda_0}{\sqrt{\epsilon_{eff}}} \quad (2)$$

$$\epsilon_{eff} = \frac{\epsilon_r + 1}{2} + \frac{\epsilon_r - 1}{2} \left[1 + 12 \frac{h}{w} \right]^{-1/2} \quad (3)$$

where λ_g and λ are the wavelength in the medium and in the free space, respectively; ϵ_{eff} is the effective relative dielectric constant.

Therefore the notch frequency, f_{notch} is given by

$$f_{notch} \approx \frac{c}{2 * L_{slot} \sqrt{\epsilon_{eff}}} \quad (4)$$

Using curve fitting, the relationship between the notched frequency, f_{notch} and the total length of the half wavelength of a slot resonator

can be approximated by second order polynomial as follows,

$$L_t \approx 0.51 (f_{notch})^2 - 9.7 (f_{notch}) + 55 \quad 3 \leq f_{notch} \leq 11 \quad (5)$$

where L_t in mm and f_{notch} in GHz.

The proposed formula to calculate the notched frequency is validated by comparing the calculated results with the simulated results obtained from the EM simulator. Figure 5 shows the comparison between calculated and simulated results of the notched frequency for various total slot lengths of the open ring slot as well as the π -shaped slot. The simulated range of lower and upper limits of the open ring slot is between 21.0 and 30.4 mm. Consequently, the formula is valid when the range of the lower and upper limits of f_{notch} between 3.5 and 4.4 GHz. On the other hand, the simulated range of the lower and upper limits of $L_{\pi t}$ is between 9.4 and 18.4 mm, which corresponding to f_{notch} between 5.2 and 10.5 GHz.

The proposed formula can be used for fast determination of the band-notch responses of half wavelength resonators which describe the influences of these notched structures on the corresponding notched frequencies in the UWB range from 3 to 11 GHz.

4. RESULTS AND DISCUSSIONS

The simulations of the antenna are performed using CST Microwave Studio commercial software. The measured and simulated results of the VSWR for the proposed antenna are illustrated in Figure 6. The simulated result obtained by HFSS software is also included for comparison. It is apparent that the proposed antenna can cover an ultra wide frequency band of 2.7–17 GHz for VSWR < 2, with dual notched bands of 3.3–3.8 GHz for WiMAX system and 5.0–6.1 GHz for WLAN system, respectively. The discrepancy in VSWR between the simulated and the measured results may be attributed to the fabrication tolerance and facilities. Due to the small size of the antenna it is difficult to do alignment between the top and bottom sides of the antenna. Also, some errors may be contributed from the spatial closeness between the connector and the radiating slot as well as the shunt stub. In high frequencies there are little differences between the simulated results obtained from the CST and HFSS simulators. Figure 7 shows the input impedance of the proposed antenna with and without open shunt stub. It is apparent that the input impedance of the proposed antenna with open shunt stub is more adjusted and better than that of the antenna without the open shunt stub, which enhance the impedance bandwidth of the antenna.

In order to better understand the mechanism of the band-notched characteristics, the simulated current distributions at the centers

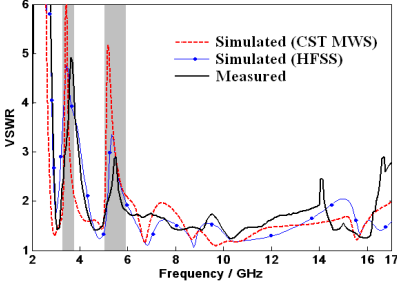


Figure 6. Measured and simulated VSWR as a function of frequency of the proposed antenna.

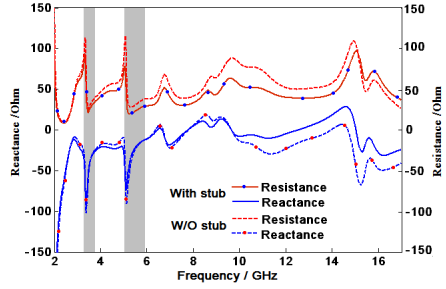


Figure 7. Simulated input impedance versus frequency of the proposed antenna with and without open shunt stub.

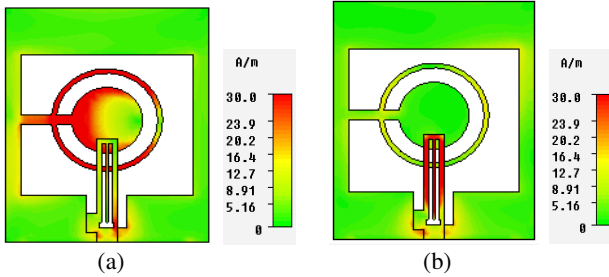


Figure 8. Surface current distributions of the proposed antenna at notched frequencies. (a) 3.55 GHz. (b) 5.55 GHz.

of notched-frequency bands of 3.55 and 5.55 GHz for the proposed antenna are investigated and shown in Figure 8. It can be seen that the surface currents at 3.55 GHz mainly concentrated along the open ring slot. The resonant surface current at 5.55 GHz mainly distributed along the π -shaped slot. These current distributions cause the antenna to be nonresponsive at the corresponding notch frequencies.

Figure 9 shows the normalized far-field radiation patterns of E_θ and E_ϕ in the y - z (E -plane) and x - z (H -plane) planes of the proposed antenna at frequencies 3.1, 4.5 and 7.5 GHz. It is observed that the simulated patterns exhibit a relatively omnidirectional radiation in the x - z plane at these frequencies; whereas, simulated patterns in the y - z plane illustrate radiations look like E -plane radiation pattern of a vertical dipole.

The simulated peak gain and the radiation efficiency of the

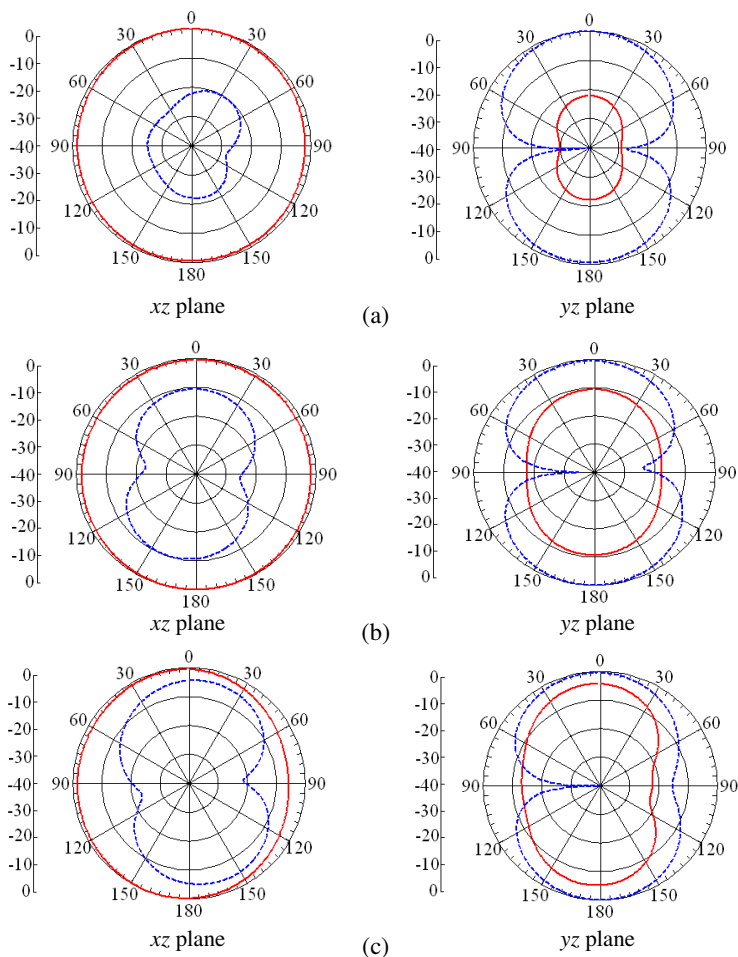


Figure 9. Simulated radiation patterns of E_θ (dashed line) and E_ϕ (solid line) in the y - z and x - z planes of the proposed antenna at different frequencies. (a) 3.1 GHz. (b) 4.5 GHz. (c) 7.5 GHz.

proposed antenna are shown in Figure 10. Stable gain with an average of about 4 dBi is obtained throughout the operating band. Two sharp dips in the antenna gain can be observed in the notched-frequency bands in the vicinity of 3.55 and 5.55 GHz. This result presents that the proposed antenna has good dual band-notched characteristics at WiMAX and WLAN systems. The radiation efficiency is almost 75% overall the whole frequency band excluding the two rejected bands.

The proposed UWB antenna fulfills all the critical requirements

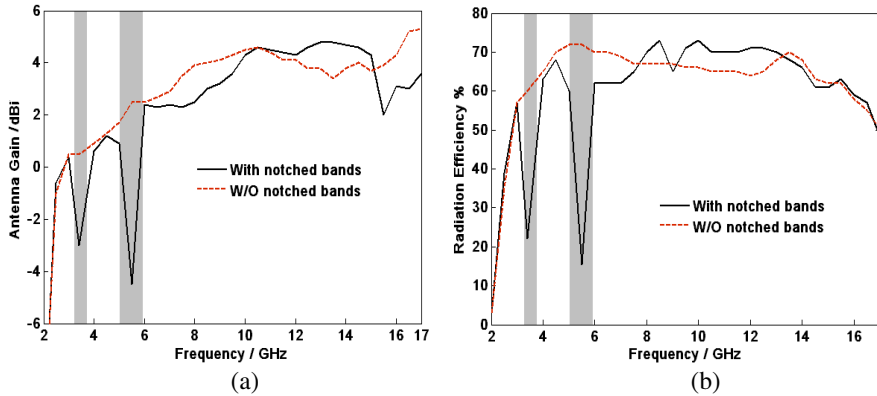


Figure 10. (a) Simulated antenna peak gain, and (b) radiation efficiency versus frequencies for the proposed antenna with and without the resonating slots.

including high radiation efficiency, low profile small size, stable radiation patterns and relatively constant gain. In addition, the dual notched-frequency bands at 3.3–3.8 GHz and at 5.0–6.1 GHz can successfully block out the whole WiMAX and WLAN bands, respectively. Therefore, the potential interferences between the proposed UWB antenna and these systems can be excluded or reduced to minimum. In the other hand, the antenna bandwidth is more enhanced in the higher frequency band, which added more benefit to the proposed antenna to be used in other applications.

In practice, the proposed antenna is suitable to integrate with compact UWB communication systems. As compared with the reported antennas in the literature, the proposed antenna with proximity-fed technique provides good behavior in a similar working frequency band with less complexity and smaller size. Table 1 illustrates comparison between the behaviors of proposed antenna with those similar designs of slot antenna configurations as given in the literature with microstrip-fed as well as CPW-fed techniques.

5. EQUIVALENT CIRCUIT SYNTHESIZED

For further comprehension of the proposed antenna performance, a SPICE-compatible circuit modeling method is applied to the proposed antenna to establish its lumped-element equivalent circuit model. The method is described as follows: First, the response of the input admittance/impedance of the proposed antenna obtained by

Table 1. Comparisons between the proposed antenna and the other similar antennas in literature.

Approach	Feeding Type	Overall Size (L X W) (mm ²)	Impedance BW (VSWR≤2)	Notched band(s), Notched Gain, Techniques
Proposed	Proximity-FED	20 X 25	2.7–17 GHz	3.3–3.8 GHz, –3.2 dBi An Open ring slot etched off the patch 5.0–6.1 GHz, –4.5 dBi A π-shaped slot etched off the feeding line
Reference [5]	CPW-FED	40 X 30	2–11 GHz	3.3–3.7 GHz, –6.5 dBi A L-shape branch is attached to slotted ground plane 5.15–5.825 GHz, –1 dBi A L-shape branch is attached to slotted ground plane
Reference [6]	CPW-FED	39 X 35	2.6–14.34 GHz	3.3–3.7 GHz, –4 dBi A C-shaped slot etched inside exciting stub 5.04–6 GHz, –8dBi A pair of open-circuit stubs symmetrically added at the edge of the slot
Reference [7]	Microstrip-FED	31 X 31	2–11 GHz	3.3–4 GHz, –4.5 dBi A pair of L-shaped slots etched on either sides of the ground plane 5–5.7 GHz, –4.3 dBi Modified a pair of L-shaped slots on either side of the ground plane
Reference [13]	Microstrip-FED	40 X 30	3.1–10.6 GHz	3.15–3.90 GHz, –10.38 dBi A C-shaped slot etched off feeding line 5.10–5.95 GHz, –4.41 dBi A parasitic strip is printed in circular slot

simulation or measurement is estimated in the frequency range of interest. There is no rule for the number of frequency points that should be sampled, but it is suggested to use no less than 100 points. Second, the simulated response of the input admittance/impedance is fitted by means of the Vector Fitting (VF) technique using MATLAB RF Toolbox “rationalfit” to obtain a modified rational function [28]. Finally, the rational function is converted into a SPICE-compatible equivalent circuit and the synthesized component values are obtained.

The modified rational function approximation of a certain frequency domain response $F(s)$ using VF technique can be expressed as [29]:

$$F(s) = \left(\sum_{k=1}^N \frac{res_k}{s - p_k} + D \right) e^{-s \times Delay} \tag{6}$$

where res_k and p_k denote the k -th residues and poles, respectively,

which are either real quantities or come in complex conjugate pairs of N identical sets of poles (order of approximation). $s = j\omega$ represents the complex frequency, and D and Delay are constant terms which are real. All coefficients in Eq. (6) should be calculated so that an approximation of $F(s)$ is obtained over a given frequency interval. In general, VF solves this problem sequentially as a linear problem in two stages: poles identification and residues identification, both with known poles. The details of this procedure can be found in [30].

Without loss of generality, in this paper $F(s)$ is applied to the admittance-type function, $Y(s)$, for the proposed antenna. The delay element is always equal to zero because the presentation of the antenna has only one port [29]. The constant term D is optional and can be synthesized with a resistance, R_0 whose value is calculated as

$$R_0 = \frac{1}{D} \quad (7)$$

The equivalent circuit for the remaining parts of $F(s) = \sum_{k=1}^N \frac{res_k}{s-p_k}$ can be evaluated as [31].

– Each real pole, $F(s) = \frac{res_k}{s-p_k}$, (for $k = 1$ to N) gives an RL -branch

$$L_k = \frac{1}{res_k}, \quad R_k = -\frac{p_k}{res_k} \quad (8)$$

– Each complex conjugate pair, $F(s) = \frac{res_1}{s-p_1} + \frac{res_2}{s-p_2}$, gives an RLC -branch

$$\begin{aligned} L &= \frac{1}{res_1 + res_2} \\ C &= \frac{res_1 + res_2}{p_1 p_2 + \left[-(p_1 + p_2) + \frac{res_1 p_2 + res_2 p_1}{res_1 + res_2} \right] \times \left[\frac{res_1 p_2 + res_2 p_1}{res_1 + res_2} \right]} \\ R &= \frac{1}{res_1 + res_2} \times \left[-(p_1 + p_2) + \frac{res_1 p_2 + res_2 p_1}{res_1 + res_2} \right] \\ R' &= -\frac{1}{C} \frac{res_1 + res_2}{res_1 p_2 + res_2 p_1} \end{aligned} \quad (9)$$

The procedures to extract such elements can be synthesized as described in [32].

The process can be started by a certain value of relative error which corresponds to a certain value of N which is used as a minimum order of approximation, say $N = 2$. The complete synthesis SPICE-compatible equivalent circuit for the input admittance of an antenna can provide either two real poles or one complex pair which can be modeled as presented in Figure 11 (a pole of order $N = 1$ is called

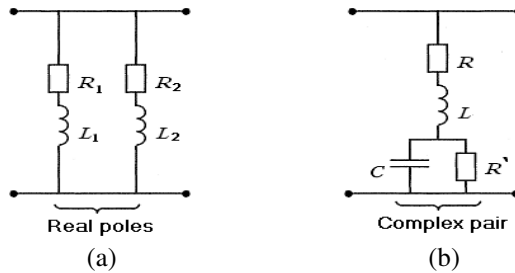


Figure 11. SPICE-compatible equivalent circuit for the input admittance of an antenna for $N = 2$ and $D = 0$. (a) For two real poles. (b) For one complex conjugate pair.

a simple pole). Increasing the order of approximation N , will increase number of either resultant real poles or complex pairs.

Now use MATLAB RF Toolbox “rationalfit” to obtain a modified rational function. First, we compute the relative error as a vector containing the dependent values of the data to be fitted. The default tolerance is -10 dB. If the model does not fit the original data within the specified tolerance, we increase the relative error-fitting tolerance, which increases the order of approximation N and increase the number of either the resultant real poles or the complex pairs.

For instant, if the process is started with its default value relative error = -10 dB, the $Y(s)$ will only fitted with six complex conjugate ($N = 12$) which causes the resulting approximation for $Y(s)$ be extremely inaccurate. Consequently the root mean square error becomes large. For the proposed antenna the relative error-fitting tolerance after recalculation is reached to -40 dB that increase the order of approximation to 28 and a very accurate approximation is achieved. The rational function approximation of $Y(s)$ using VF (poles and residues) is listed in Table 2. The fitting procedure provides 14 complex conjugate pairs. Figure 12 shows the magnitude and phase errors between the simulated results of the input admittance and the results using “rationalfit” procedure. The figure illustrates very good approximation and the root-mean-square error of the magnitude is nearly $4.877e-004$. Table 3 shows the components values for the equivalent circuit of the proposed antenna. The equivalent circuit model for the input admittance of the proposed antenna for $N = 28$ and relative error = -40 dB is synthesized as shown in Figure 13(a). The VSWR characteristics of the proposed antenna are shown in Figure 13(b), in which very good agreement between simulated results and those obtained from the equivalent circuit modeling is observed.

Table 2. The rational function approximation for the input admittance $Y(s)$ of the proposed antenna (when $D = 0$).

Type and No. of poles	Poles (1e+11)	Residues (1e+9)
Complex 1	$-0.4231 \pm 1.0943i$	$1.8093 \pm 2.0516i$
Complex 2	$-0.0139 \pm 0.9713i$	$0.0087 \pm 0.0034i$
Complex 3	$-0.1325 \pm 0.8921i$	$0.0608 \pm 0.5051i$
Complex 4	$-0.0503 \pm 0.7439i$	$0.0170 \pm 0.0048i$
Complex 5	$-0.0392 \pm 0.6377i$	$0.0219 \pm 0.0103i$
Complex 6	$-0.0170 \pm 0.5570i$	$0.0117 \pm 0.0080i$
Complex 7	$-0.0659 \pm 0.4759i$	$0.2793 \pm 0.0193i$
Complex 8	$-0.0273 \pm 0.4079i$	$0.0308 \pm 0.0648i$
Complex 9	$-0.0294 \pm 0.3533i$	$0.0456 \pm 0.0077i$
Complex 10	$-0.0119 \pm 0.3205i$	$-0.0148 \pm 0.0139i$
Complex 11	$-0.0052 \pm 0.0839i$	$0.0430 \pm 0.0156i$
Complex 12	$-0.0502 + 0.2423i$	$0.0803 \pm 0.0108i$
Complex 13	$-0.0087 \pm 0.1703i$	$0.0174 \pm 0.0116i$
Complex 14	$-0.0075 \pm 0.2146i$	$-0.0095 \pm 0.0006i$

It is noted that the VF technique guarantees stable poles and also enforcing passivity. With stable poles and passivity enforced, the resulting equivalent circuit may still have unphysical circuit elements (negative resistance, capacitance and inductance), as shown in Table 3, even though we use low order of approximation. But we will never get an unstable simulation since the circuit as a whole will always consume power, whatever we connect to it [33]. However, numbers and values of the negative elements depend on the frequency range of the function to be fitted as well as the order of approximation used in that fitting. Higher accuracy can be easily involved by increasing the order of the approximation. But the complexity of the equivalent circuit will also be increased at the same time. For instant, due to ultra-wide bandwidth, the resulting equivalent circuit may still have more negative circuit elements with large values, but the whole equivalent circuit will be passive. A circuit having negative capacitance/inductance can present,

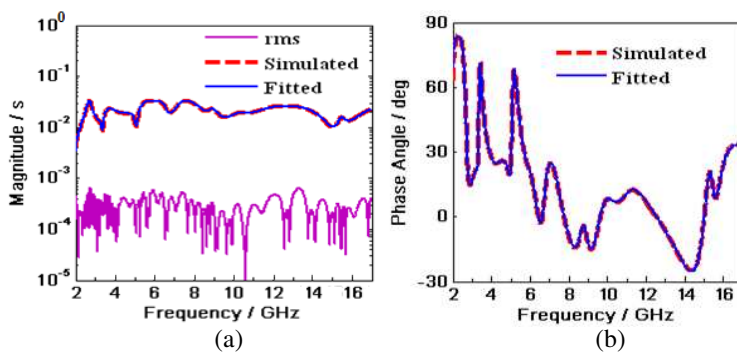


Figure 12. Comparison of the input admittance for the proposed antenna between the simulate results and the “rationalfit” procedure results. (a) Magnitude functions. (b) Phase angles.

Table 3. Synthesized components values for the proposed antenna.

Type and No. of poles	L (H)	R (Ω)	C (F)	R' (Ω)
Complex 1	2.76e-10	45.98238	1.32e-13	-92.4987
Complex 2	5.75e-08	2238.108	1.60e-15	-17249.9
Complex 3	8.22e-09	-5987.64	2.18e-16	6076.303
Complex 4	2.94e-08	758.3636	5.71e-15	-11120.5
Complex 5	2.28e-08	771.3169	8.83e-15	-4361.91
Complex 6	4.28e-08	1700.955	5.14e-15	-5351.45
Complex 7	1.79e-09	17.69234	2.46e-13	1234.426
Complex 8	1.62e-08	-1349.12	6.82e-15	1655.607
Complex 9	1.10e-08	-33.0948	7.11e-14	1580.878
Complex 10	-3.37e-08	-1050.51	-1.54e-14	2256.993
Complex 11	1.16e-08	41.27822	1.08e-12	-367.043
Complex 12	6.22e-09	10.94282	2.69e-13	448.8052
Complex 13	2.88e-08	352.2087	8.29e-14	-1148.25
Complex 14	-5.26e-08	-113.187	-4.11e-14	36868.79

by duality, another inductive/capacitive element. In a negative capacitance the current will be 180° opposite in phase to the current in a positive capacitance. Instead of leading the voltage by 90° it will lag the voltage, as in an inductor. Therefore a negative

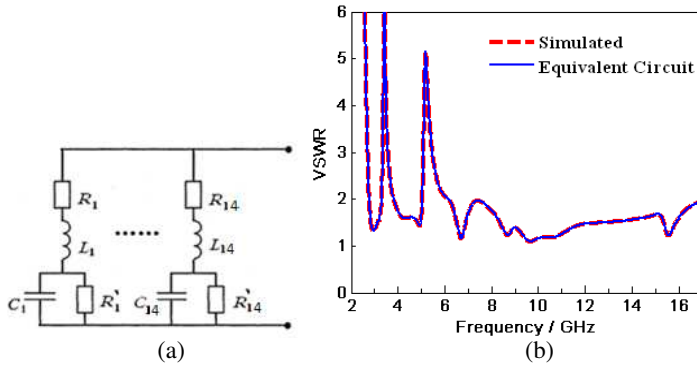


Figure 13. (a) Equivalent circuit synthesis of the proposed dual band-notched UWB antenna for $N = 28$ and $D = 0$. (b) VSWR characteristic as a function of frequency for the proposed antenna.

capacitance acts like an inductance in which the impedance has a reverse dependence on frequency; decreasing instead of increasing acts like a real inductance. Similarly a negative inductance acts like a capacitance that has impedance which increases with frequency [34].

Finally, the major limitation of this approach is the fact that this technique is not systematic. In other words, the method does not contain a physics-based approach. Nevertheless, it is stressed that this technique can be used as a tool to aid engineers in designing an actual passive circuit that can be used to mimic the scattering parameter response of a UWB antenna [35]. In spite of this, good agreement between the simulated results and the fitted data with acceptable equivalent model behaviors is obtained. The validity of the modeling method is verified, and high accurate results are achieved. The provided circuit model is useful to consider the effect of the proposed antenna when integrated with the whole communication system. It also helps designers to predict the communication system performances.

6. CONCLUSIONS

In this paper, a miniaturized and compact UWB printed slot antenna with dual band-notched is presented. The antenna is based on microstrip structure with an open shunt stub, proximity-fed a circular disk radiating patch. The proposed antenna achieves UWB conditions. It operates within a band from 2.7 to 17 GHz. The proposed antenna is designed to have two band-notches to avoid the undesirable

interferences with the 3.5 GHz band for WiMAX systems and the 5.5 GHz band for WLAN systems with a simple structure. The first notch is achieved by etching an open ring slot in the circular disk patch. Whereas the other notch is achieved by a π -shaped slot etched off the feeding line. The parameters and the characteristics of the antenna are given. A detailed study of the influences of different parameters was carried out. Curve fitting formulations are obtained to describe the influences of the notches resonators on the corresponding notched frequencies by using first and second order polynomial. Moreover, with the help of VF technique, a SPICE-compatible lumped-element equivalent circuit modeling for the proposed antenna is established. The proposed antenna is fabricated, and the measured data of the VSWR showed a good agreement with the simulated results along with the equivalent circuit modeling results. The proposed antenna featured suitable radiation patterns with good gain flatness over the UWB frequency band excluding the two rejected bands.

REFERENCES

1. Federal Communications Commission Revision of Part 15 of the Commission's Rule Regarding Ultra-Wideband Transmission System, FCC, First Report and Order FCC, 02-48, 2002.
2. Khaled, E. E. M., A. A. R. Saad, and D. A. Salem, "A proximity-fed annular slot antenna with different a band-notch manipulations for ultra-wideband applications," *Progress In Electromagnetics Research B*, Vol. 37, 289-306, 2012.
3. Dissanayake, T. and K. P. Esselle, "Prediction of the notch frequency of slot loaded printed UWB antennas," *IEEE Trans. Antennas Propag.*, Vol. 55, No. 11, part: 2, 3320-3325, Nov. 2007.
4. Abbosh, M., M. E. Bialkowski, J. Mazierska, and M. V. Jacob, "A planar UWB antenna with signal rejection capability in the 4-6 GHz Band," *IEEE Micro. Wireless Comp. Lett.*, Vol. 16, No. 5, 278-280, May 2006.
5. Liu, X., Y. Yin, P. Liu, J. Wang, and B. Xu, "A CPW-Fed dual band-notched UWB antenna with a pair of bended dual-L-shape parasitic branches," *Progress In Electromagnetics Research*, Vol. 136, 623-634, 2013.
6. Mandal, T., and S. Das, "An optimal design of CPW-fed UWB aperture antennas with WiMAX/WLAN notched band characteristics," *Progress In Electromagnetics Research C*, Vol. 35, 161-175, 2013.
7. Li, W. M., T. Ni, S. M. Zhang, J. Huang, and Y. C. Jiao, "UWB

- printed slot antenna with dual band-notched characteristic," *Progress In Electromagnetics Research Letters*, Vol. 25, 143–151, 2011.
8. Li, C. M., and L. H. Ye, "Improved dual band-notched UWB slot antenna with controllable notched bandwidths," *Progress In Electromagnetics Research*, Vol. 115, 477–493, 2011.
 9. Li, W.-M., T. Ni, T. Quan, and Y.-C. Jiao, "A compact CPW-fed UWB antenna with WiMAX-band notched characteristics," *Progress In Electromagnetics Research Letters*, Vol. 26, 79–85, 2011.
 10. Sun, J.-Q., X.-M. Zhang, Y.-B. Yang, R. Guan, and L. Jin, "Dual band-notched ultra-wideband planar monopole antenna with M- and W-slots", *Progress In Electromagnetics Research Letters*, Vol. 1, 1–8, 2010.
 11. Tu, S., Y. C. Jiao, Y. Song, B. Yang, and X. Z. Wang, "A novel monopole dual band-notched antenna with tapered slot for UWB applications," *Progress In Electromagnetics Research Letters*, Vol. 10, 49–57, 2009.
 12. Zhang, J., S. W. Cheung, and T. I. Yuk, "CPW-coupled-elliptical monopole UWB antenna with dual-band notched characteristic," *PIERS Proceedings*, 823–827, Kuala Lumpur, Malaysia, March 27–30, 2012.
 13. Gao, G. P., Z. L. Mei, and B. N. Li, "Novel circular slot UWB antenna With dual band-notched characteristic," *Progress In Electromagnetics Research C*, Vol. 15, 49–63, 2010.
 14. Yang, G., Q.-X. Chu, and T.-G. Huang, "A compact UWB antenna with sharp dual band-notched characteristics for lower and upper WLAN band," *Progress In Electromagnetics Research C*, Vol. 29, 135–148, 2012.
 15. Mishra, S. K. and J. Mukherjee, "Compact printed dual band-notched U-shape UWB antenna," *Progress In Electromagnetics Research C*, Vol. 27, 169–181, 2012.
 16. Lui, W. J., C. H. Cheng, and H. B. Zhu, "Compact frequency notched ultra-wideband fractal printed slot antennas," *IEEE Micro. Wireless Comp. Lett.*, Vol. 16, No. 4, 224–226, Apr. 2006.
 17. Lui, W. J., C. H. Cheng, Y. Cheng, and H. Zhu, "Frequency notched ultra-wideband microstrip Slot antenna with fractal tuning stub," *Electron. Lett.*, Vol. 41, No. 6, 294–296, Mar. 2005.
 18. Karmakar, A., S. Verma, M. Pal, and R. Ghatak, "An ultra wideband monopole antenna with multiple fractal slots with dual band rejection characteristics," *Progress In Electromagnetics*

- Research C*, Vol. 31, 185–197, 2012.
19. Ali, J. K., A. J. Salim, A. I. Hammoodi, and H. Alsaedi, “An ultra-wideband printed monopole antenna with a fractal based reduced ground plane,” *PIERS Proceedings*, 613–617, Moscow, Russia, August 2012.
 20. Kim, D.-O., N.-I. Jo, D.-M. Choi, and C.-Y. Kim, “Design of the ultra-wideband antenna with 5.2 GHz/5.8 GHz band rejection using rectangular split-ring resonators (SRRS) loading,” *Journal of Electromagnetic Waves and Applications*, Vol. 23, No. 17–18, 2503–2512, 2009.
 21. Kim, J., C. S. Cho, and J. W. Lee, “5.2 GHz notched ultra-wideband antenna using slot-type SRR,” *Electron. Lett.*, Vol. 42, 315–316, 2006.
 22. Liu, L., Y. Z. Yin, C. Jie, J. P. Xiong, and Z. Cui, “A compact printed antenna using slot-type CSRR for 5.2GHz/5.8GHz band-notched UWB application,” *Microw. Opt. Techn. Lett.*, Vol. 50, 3239–3242, 2008.
 23. Yin, X. C., C. L. Ruan, C. Y. Ding, and J. H. Chu, “A compact ultra-wideband microstrip antenna with multiple notches,” *Progress In Electromagnetics Research*, Vol. 84, 321–332, 2008.
 24. Lai, H.-Y., Z.-Y. Lei, Y.-J. Xie, G.-L. Ning, and K. Yang, “UWB antenna with dual band rejection for WLAN/WiMAX bands using CSRRs,” *Progress In Electromagnetics Research Letters*, Vol. 26, 69–78, 2011.
 25. Zhang, Y., W. Hong, C. Yu, Z.-Q. Kuai, Y.-D. Don, and J.-Y. Zhou, “Planar ultrawideband antennas with multiple notched bands based on etched slots on the patch and/or split ring resonators on the feed line,” *IEEE Trans. Antennas Propag.*, Vol. 56, No. 9, 3063–3068, Sept. 2008.
 26. Xu, F., Z. X. Wang, X. Chen, and X.-A. Wang, “Dual band-notched UWB antenna based on spiral electromagnetic-bandgap structure,” *Progress In Electromagnetics Research B*, Vol. 39, 393–409, 2012.
 27. Saad, A. A. R., D. A. Salem, and E. E. M. Khaled, “5.5 GHz notched ultra-wideband printed monopole antenna characterized by electromagnetic band gap structures,” *International Journal of Electronics and Communication Engineering (IJECE)*, Vol. 1, No. 1, 1–12, Aug. 2012.
 28. MATLAB Program, The MathWorksTM, Inc., Version 7.10.0.499 (R2010a), Feb. 2010.

29. Zeng, R. and J. Sinsky, "Modified rational function modeling technique for high speed circuits," *IEEE MTT-S Inter. Microw. Symp. Digest*, 1951–1954, San Francisco, Jun. 2006.
30. Gustavsen, B. and A. Semlyen, "Rational approximation of frequency domain responses by vector fitting," *IEEE Trans. Power Delivery*, Vol.14, 1052–1061, Jul. 1999.
31. Ren, W., "A new circuit modeling methodology for RFID antennas with vector fitting technique," *6th Intern. Conf. Wireless Comm. Networking and Mobile Computing (WiCOM)*, 1–4, Chengdu, China, Sept. 2010.
32. Antonini, G., "SPICE equivalent circuits of frequency-domain responses," *IEEE Trans. Electrom. Compatibility*, Vol. 45, No. 3, 502–512, Aug. 2003.
33. Gustavsen, B. and A. Semlyen, "Enforcing passivity for admittance matrices approximated by rational functions," *IEEE Trans. Power System*, Vol. 16, 97–104, Feb. 2001.
34. Hickman, I., *Analog Circuits Cookbook*, 2nd Edition, Newnes, New York, 1999.
35. DeJean, G. R. and M. M. Tentzeris, "The application of lumped element equivalent circuits approach to the design of single-port microstrip antennas," *IEEE Trans. Antennas Propag.*, Vol. 55, No. 9, 2472–2468, Sept. 2007.